Triggering, bypass transition and the effect of noise on a linearly stable thermoacoustic system

I. Waugh[a,*], Matthias Geuß[b], M. Juniper[a]

[a]*Cambridge University Engineering Department, Trumpington Street,Cambridge, CB2 1PZ, United Kingdom, Fax: +44 1223 332662.*
[b]*Technische Universität, München*

Abstract

This paper explores the analogy between triggering in thermoacoustics and bypass transition to turbulence in hydrodynamics. These are both mechanisms through which a small perturbation causes a system to develop large self-sustained oscillations, despite the system being linearly stable. For example, it explains why round pipe flow (Hagen-Poiseuille flow) can become turbulent, even though all its eigenvalues are stable at all Reynolds numbers.

In hydrodynamics, bypass transition involves transient growth of the initial perturbation, which arises due to linear non-normality of the stability operator, followed by attraction towards a series of unstable periodic solutions of the Navier-Stokes equations, followed by repulsion either to full turbulence or re-laminarization. This paper shows that the triggering process in thermoacoustics is directly analogous to this. In thermoacoustics, the linearized stability operator is also non-normal and also gives rise to transient growth. The system then evolves towards an unstable periodic solution of the governing equations, followed by repulsion either to a stable periodic solution or to the zero solution. The paper demonstrates that initial perturbations that have higher amplitudes at low frequencies are more effective at triggering self-sustained oscillations than perturbations that have similar amplitudes at all frequencies.

This paper then explores the effect that different types of noise have on triggering. Three types of noise are considered: pink noise (higher amplitudes at low frequencies), white noise (similar amplitudes at all frequencies) and blue noise (higher amplitudes at high frequencies). Different amplitudes of noise are applied, both as short bursts and continuously. Pink noise is found to be more effective at causing triggering than white noise and blue noise, in line with the results found in the first part of the paper.

In summary, this paper investigates the triggering mechanism in thermoacoustics and demonstrates that some types of noise cause triggering more effectively than others.

Keywords: Thermoacoustics, Non-normality, Triggering, Transient growth, Unstable attractors

*Corresponding author

[1]Length 5780 words as determined by method 2. Submitted to 110: IC Engine and Gas Turbine Combustion

1. Introduction

In some linearly-stable thermoacoustic systems, self-sustained oscillations can be triggered by perturbations with amplitudes similar to the background noise level [1, Ch1 §IV]. This is known as triggering. In some linearly-stable hydrodynamic systems, turbulence can be triggered by perturbations with a similarly small amplitude [2]. This is known as bypass transition to turbulence. An analogy between the two has been suggested [1, Ch1 §IV] but has not yet been investigated fully. While it is clear that non-linear effects are important, it has only recently been shown that non-normal effects are also influential [3, 4].

In hydrodynamics, bypass transition can be divided into five stages [2]. The first stage is initiation of small perturbations to the flow. The second stage is linear amplification of these perturbations due to non-normal growth. The third stage is non-linear saturation towards a new unstable quasi-steady periodic state. The fourth stage is growth of secondary instabilities on top of this periodic base flow. The fifth stage is breakdown to turbulence, where non-linearities and/or symmetry-breaking instabilities excite an increasing number of scales in the flow.

The second, third and fourth stages can also be considered in terms of dynamical systems [5, 6, 7]. A boundary in state space is identified between trajectories that decay to a laminar solution and trajectories that evolve to a turbulent solution. This is known as the 'edge of chaos'. Trajectories from certain regions of state space are attracted towards this boundary. Those that are attracted from lower energy states exhibit the non-normal transient growth identified in stage 2. The boundary itself corresponds to the unstable periodic state identified in stage 3. In hydrodynamics, this boundary contains several heteroclinic saddle points and at least one local relative attractor, each corresponding to a periodic travelling wave solution [7]. The saddle points have at least two unstable eigenvalues in the boundary. This means that trajectories enter along their stable manifolds and exit along their unstable manifolds without leaving the boundary. The state therefore wanders from the vicinity of one travelling wave solution to the vicinity of another until it reaches a local relative attractor. The local relative attractor (an unstable attractor), has just one unstable eigenvalue so trajectories enter from all directions along the boundary but exit perpendicular to the boundary. Whether this trajectory then evolves towards a laminar solution or towards a turbulent solution, corresponding to stage 5 above, depends on the direction in which it exits the boundary. This, in turn, depends very sensitively on its initial position in phase space at stage 1.

In thermoacoustics, the analogous boundary is between trajectories that decay to zero, which are analogous to the laminar solution, and trajectories that evolve to high amplitude self-sustained oscillations, which are analogous to the turbulent solution. Recent studies, such as [8], have shown that a trajectory starting from this boundary can evolve to the high amplitude state. If the analogy is appropriate, however, trajectories from other regions of state space will be attracted towards this boundary and then be repelled either to a high or a low amplitude state. Thermoacoustic systems, like many hydrodynamic systems, are non-normal [3, 9], meaning that this attraction can be from states with lower energy than the boundary.

The first aim of this paper is to explore the analogy between triggering in thermoacoustics and bypass transition in hydrodynamics. The second aim is, in light of this link, to investigate the effect that different types of noise have on triggering in a simple thermoacoustic system.

2. Governing equations

The thermoacoustic system examined in this paper is identical to that studied by Refs. [3, 10], which contain a complete description. In summary, it is a tube of length L_0 in which a hot wire is placed $\tilde{x}_f$ from one end; §6.2 of [11]. A base flow is imposed through the tube with velocity u_0. The non-dimensional governing equations for momentum and energy are:

$$\frac{\partial u}{\partial t} + \frac{\partial p}{\partial x} = 0, \tag{1}$$

$$\begin{aligned} &\frac{\partial p}{\partial t} + \frac{\partial u}{\partial x} + \zeta p - \beta\delta(x - x_f)\times \quad \dots \\ &\left(\left|\frac{1}{3} + u_f(t-\tau)\right|^{\frac{1}{2}} - \left(\frac{1}{3}\right)^{\frac{1}{2}}\right) \quad = \quad 0, \end{aligned} \tag{2}$$

The system has four control parameters: ζ, which models the damping; β, which encapsulates all the information about the hot wire, base flow and ambient conditions; τ, which is the time delay between the velocity at the wire and the subsequent heat release and x_f, which is the position of the wire. The heat release parameter, β, is equivalent to $k/\gamma M$ in [3].

For the system examined in this paper, $\partial u/\partial x$ and p are both set to zero at the ends of the tube. These boundary conditions are enforced by choosing an appropriate basis set:

$$u(x,t) \quad = \quad \sum_{j=1}^{N} \eta_j(t)\cos(j\pi x), \tag{3}$$

$$p(x,t) \quad = \quad -\sum_{j=1}^{N} \left(\frac{\dot{\eta}_j(t)}{j\pi}\right)\sin(j\pi x), \tag{4}$$

where the relationship between η_j and $\dot{\eta}_j$ has not yet been specified. In this Galerkin discretization, all the modes are orthogonal. It is important to point out that these modes are not, in general, the eigenmodes of the system. They are merely the basis set into which u and p are decomposed. The governing equations then reduce to two ordinary differential equations for each mode, labelled j:

$$\frac{\mathrm{d}}{\mathrm{d}t}\eta_j - j\pi\left(\frac{\dot{\eta}_j}{j\pi}\right) = 0, \tag{5}$$

$$\begin{aligned} &\frac{\mathrm{d}}{\mathrm{d}t}\left(\frac{\dot{\eta}_j}{j\pi}\right) + j\pi\eta_j + \zeta_j\left(\frac{\dot{\eta}_j}{j\pi}\right) + 2\beta\sin(j\pi x_f)\dots \\ &\qquad \times\left(\left|\frac{1}{3} + u_f(t-\tau)\right|^{\frac{1}{2}} - \left(\frac{1}{3}\right)^{\frac{1}{2}}\right) = 0, \end{aligned} \tag{6}$$

where

$$u_f(t-\tau) = \sum_{k=1}^{N} \eta_k(t-\tau)\cos(k\pi x_f). \quad (7)$$

The state of the system is given by the amplitudes of the Galerkin modes that represent velocity, η_j, and those that represent pressure, $\dot{\eta}_j/j\pi$. These are given the notation $\mathbf{u} \equiv (\eta_1, \ldots, \eta_N)^T$ and $\mathbf{p} \equiv (\dot{\eta_1}/\pi, \ldots, \dot{\eta_N}/N\pi)^T$. The state vector of the discretized system is the column vector $\mathbf{x} \equiv (\mathbf{u}; \mathbf{p})$. The most convenient measure of the size of the perturbations is the acoustic energy per unit volume:

$$E = \frac{1}{2}u^2 + \frac{1}{2}p^2 = \frac{1}{2}\mathbf{x}^H\mathbf{x} = \frac{1}{2}||\mathbf{x}||^2, \quad (8)$$

where $||\cdot||$ represents the 2-norm.

Equations (5 - 6) can be linearized into the form $\mathrm{d}\mathbf{x}/\mathrm{d}t = \mathbf{L}\mathbf{x}$, from which it is found that $\mathbf{L}$ is non-normal [3]. (A non-normal operator satisfies $\mathbf{L}^H\mathbf{L} \neq \mathbf{L}\mathbf{L}^H$, where H denotes the Hermitian transpose.) Non-normality gives rise to linear transient growth, which is one of the main features of this paper.

3. Dynamical system behavior

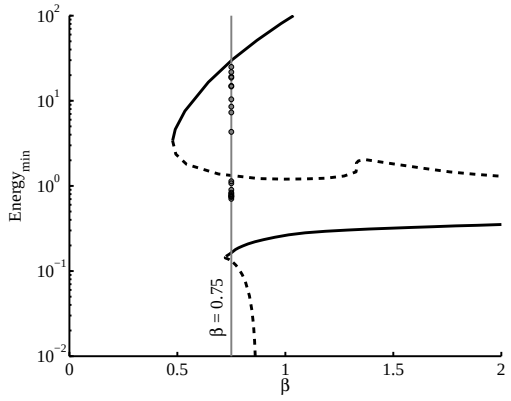

Figure 1: Bifurcation diagram for the 20-Galerkin mode system with τ of 0.02. The black points indicate the starting points for the time marching routine, taken at $\beta = 0.75$.

The bifurcation diagram in Fig. 1 shows the periodic solutions of (5 - 6) with $\zeta_j = 0.05j^2 + 0.01\sqrt{j}$, $x_f = 0.3$, $\tau = 0.02$ and $N = 20$, calculated with a bifurcation analysis tool for Delay Differential Equations [12]. Fig 1 plots the minimum acoustic energy during the periodic solution (PS) as a function of β. The Floquet multipliers of all points on the PSs are calculated to determine whether they are stable (solid lines) or unstable (dashed lines). Fig. 1 is similar to those in Refs. [1, Ch1 Fig. 1.17][8].

Even though the system is linearly stable for $0 \geq \beta \geq 0.866$, it can support a high amplitude self-sustained PS for $\beta \geq 0.478$ and a separate low amplitude PS for $\beta \geq 0.722$. The bifurcation to the lower PS at $\beta = 0.866$ is sub-critical.

The system considered in this paper is discretised with 20 Galerkin modes, as results with higher numbers of modes show

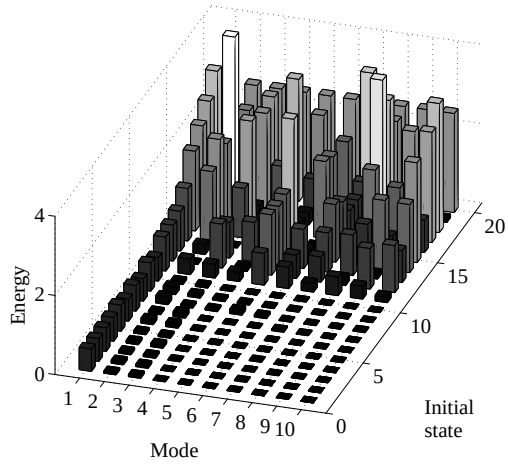

Figure 2: Energy distribution between the modes of the initial states (modes 11-20 have zero energy). Initial states 1 to 10 have low energy, initial states 11 to 20 have high energy.

negligible difference. The time-marching procedure used is similarly robust to changes in timestep.

From an initial state, the system converges to either a stable PS or the zero solution. If the initial state is close to a stable solution, the system will be attracted towards it. If the initial state is far from a stable solution, however, the system acts more interestingly. The aim of this section is to show that the unstable PSs can act as attractors during the transient phase, before repelling the trajectory towards one of the stable solutions. Such manifolds are *unstable attractors*, and are found in physical systems such as pulse-coupled oscillators [13]. These manifolds have a stable eigenvalue in at least one dimension (often more) and an unstable eigenvalue in at least one other dimension.

To demonstrate this, twenty different initial states are evolved forward in time for $\beta = 0.75$ using a 4^{th} order Runge-Kutta scheme to solve (5 - 6). These initial states have been chosen because they are all initially attracted towards the higher unstable PS. For each initial state, the total initial acoustic energy is shown as a dot on Fig. 1 and the initial energy distribution between the Galerkin modes is shown in Fig. 2. Initial states 1 to 10 have less energy than the minimum energy on the higher unstable PS. Initial states 11 to 20 have more energy than this.

For the ten initial states with low energy, the evolution of the first three Galerkin modes is plotted in Fig. 3. They initially evolve towards the same periodic trajectory in state space, which is the higher unstable PS. The energies of the first two modes grow transiently towards this while those of the third (and higher) modes decay. Although not shown in Fig. 3, the trajectories then continue alongside the unstable PS for several hundred time units before either decaying to the lower stable PS or growing to the higher stable PS [10]. It is worth noting that most of the energy in these initial states is in the first three Galerkin modes. A full analysis of the transient growth process and a non-linear adjoint looping algorithm for finding the lowest initial energy than can evolve to the higher unstable PS can

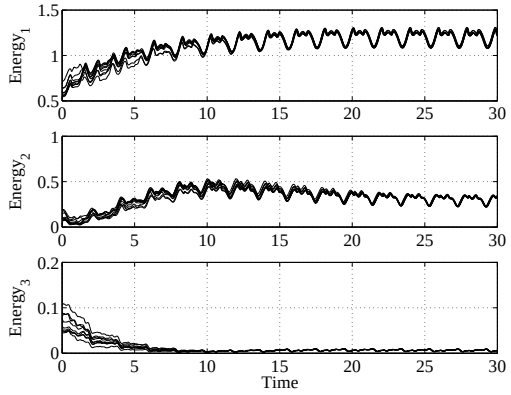

Figure 3: Time evolution from the ten low energy initial states shown in Figure 1. The acoustic energy of the first 3 Galerkin modes is plotted. Higher Galerkin modes exhibit a similar decay to the third mode.

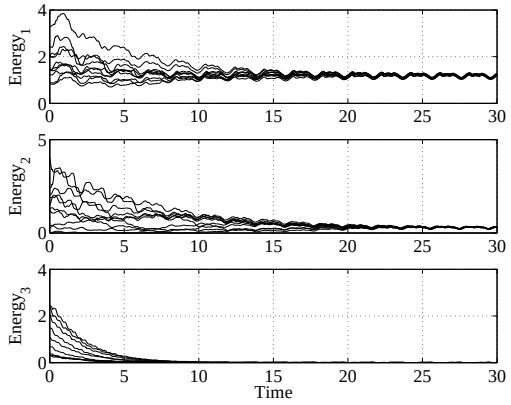

Figure 4: Time evolution from the ten high energy initial states shown in Figure 1. The acoustic energy of the first 3 Galerkin modes is plotted. Higher Galerkin modes exhibit a similar decay to the third mode.

be found in Ref. [10].

For the ten initial states with high energy, the evolution of the first three Galerkin modes is plotted in Fig. 4. They also evolve towards the higher unstable PS and, from there, either to the lower stable PS or to the higher stable PS. These initial states, however, lose a large proportion of their energy during the transient period. This can partly be explained by the damping model, $\zeta_j = 0.05j^2 + 0.01\sqrt{j}$, which damps higher modes more than lower modes. It is worth noting, however, that most of the initial states 11 to 20 start with more energy in the first three modes than initial states 1 to 10. Thus growth or decay from an initial state cannot be determined simply with an energy threshold condition.

Figs 1 to 4 demonstrate that the higher unstable PS is an unstable attractor whose basin of attraction spans a wide energy range. Trajectories that are attracted towards this PS are ultimately repelled either towards the higher stable PS or the lower stable PS. Although not shown in this paper, the same is true of the lower unstable PS [10]. The basins of attraction of both unstable PSs include regions with lower energy than the point with lowest energy on the respective unstable PS. This low energy region reaches the unstable PS via linear transient growth, which is a feature of non-normal systems. This process of attraction followed by repulsion is directly analogous to bypass transition to turbulence in hydrodynamics. Specifically, it corresponds to stages three and four in Ref. [2] and the unstable attractors are simpler versions of the 'edge of chaos' described in Refs. [5, 6, 7].

During the evolution, each Galerkin mode oscillates at its own frequency, which varies in time and is not necessarily its natural frequency. The frequency and growth rate of the first Galerkin mode, which has the highest energy, are calculated from the data in Figs. 3 and 4. They are plotted as functions of each other in Fig. 5 for initial states 1 to 10 (upper figure) and initial states 11 to 20 (lower figure). The PSs have zero growth rate. The low energy stable PS (LES) lies to the right of Fig. 5 and the high energy stable PS (HES) lies to the left. The unstable PS, to which the initial states all converge, lies in the middle. Initial states 1 to 10 have positive growth rates towards this point while initial states 11 to 20 have negative growth rates towards this point.

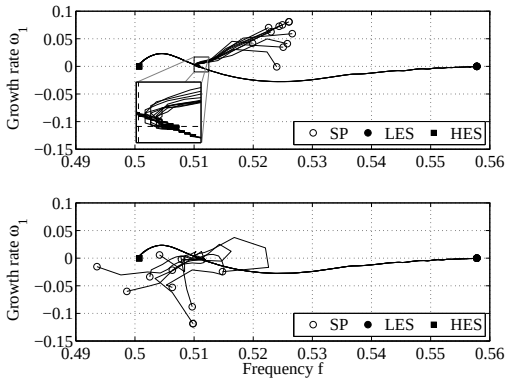

Figure 5: Evolution of the frequency and growth rate of the 1^{st} Galerkin mode from starting points (white circles) to either the high stable PS (black squares) or the low stable PS (black circles). Top frame: low energy initial states. Bottom frame: high energy initial states.

The phase portraits in Fig. 5 represent measurable outputs and can be compared with previous theoretical and experimental results. In a comprehensive theoretical and experimental study, Ref. [8] found trajectories between the unstable PS and the stable PSs that are very similar to those found in this paper. Ref. [8, Figs. 8,9], however, considered only the fundamental mode. Transient growth or transient decay towards the unstable PS cannot be modelled in a single mode system [10], which means that Ref. [8] could capture the transition away from the unstable PS but could not capture the preceding transient behaviour that is the subject of this paper.

4. Triggering with noise

The previous section assumes that the system is noiseless and deals with triggering to sustained oscillations from a given initial state. This is useful as it gives the maximum initial energy below which all states decay to the zero solution (or to the lower stable PS) in a noiseless system. This section examines the effect of forcing the system with low levels of noise, firstly as bursts of noise, secondly as continuous noise.

Noise can be divided conceptually into four types: additive noise, where a small forcing is added continually to the system; parametric noise, where coefficients in the governing equations vary; multiplicative noise, where noise amplitude is proportional to the current state of the system [14]; and modal noise, where energy is redistributed between the Galerkin modes, without any overall change in energy. This paper deals with additive noise.

At certain parameter values and forcing levels, the evolution of the system is very sensitive to the initial conditions and the forcing. This means that simulations with stochastic forcing become less clear to analyse. In order to make simulations repeatable and comparable with each other, the characteristics of the noise are determined in advance by specifying amplitudes and relative phases of the forcing of the first 10 Galerkin modes. Above the 10^{th} Galerkin mode, the response of the system to forcing is very weak and thus is not used here to form the noise profiles. This forcing signal is periodic, with period equal to that of the natural frequency of the first Galerkin mode. Three types of noise are considered: white noise, in which each mode is forced equally; pink noise, in which the lower modes are forced more than the higher modes; and blue noise, in which the higher modes are forced more than the lower modes.

4.1. Bursts of noise

Small bursts of noise in the system are examined in order to discover whether certain noise profiles are more successful than others at triggering sustained oscillations. As shown in §3, certain initial states are more successful at triggering sustained oscillations in a noiseless system. It seems logical to suppose, therefore, that the same will be true of bursts of noise.

The first noise profile is white noise, in which every Galerkin mode has equal amplitude, Fig. 6. The evolution of acoustic energy is shown in Fig. 7, in which this noise is added for 4, 5 and 6 periods. Each time unit corresponds to L_0/c_0 seconds, where L_0 is the tube length and c_0 is the speed of sound, so these bursts would be of order 10 ms in a typical Rijke tube.

The three plots in Fig. 7 capture the three types of behavior that are expected. After forcing for 4 periods (top plot), the system is not yet in the basin of attraction of the unstable PS (dashed line) and subsequently decays to the zero solution. After forcing for 5 periods, the system reaches the basin of attraction of the unstable PS, is attracted towards this solution and, from there, grows to the stable PS (solid line). After forcing for 6 periods, the system decays to the stable PS without passing via the unstable PS.

The second noise profile is shown in Fig. 8. This is a blue noise profile, in which the higher Galerkin modes are forced

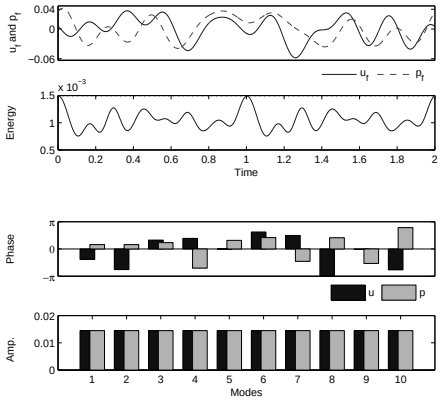

Figure 6: White noise profile in terms of the forcing signal's amplitude (top time series) and energy (bottom time series). Each Galerkin mode is forced with equal amplitude (bottom bar chart) but randomly-distributed phase (top bar chart). The noise level is quantified by the maximum energy of the signal, which is 1.49×10^{-3}.

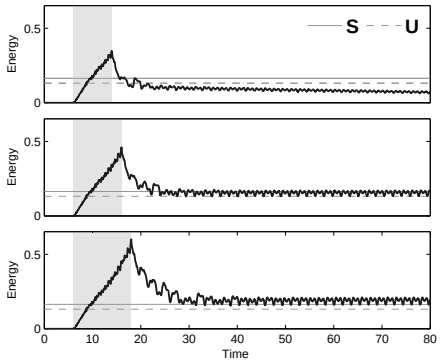

Figure 7: Evolution of the energy of the system with bursts of white noise for 4, 5 and 6 periods (shaded), showing attraction to the stable (S) and unstable (U) PSs.

with higher amplitude than the lower Galerkin modes. The maximum energy of the forcing signal is 8.6×10^{-3}, which is 2.5 times greater than that of the white noise profile. The evolution of acoustic energy is shown in Fig. 9, in which this noise is added for 4, 5 and 6 periods.

The three plots in Fig. 9 capture the same three types of behavior seen for the white noise. The blue noise, however, requires much higher energy than the white noise to trigger self-sustained oscillations. This is expected from the results in §3, in which it was shown that a system reaches sustained oscillations from a lower initial energy when that energy is mainly in the lower Galerkin modes. Although not shown here, similar simulations with pink noise show that, as expected, less energy (6.9×10^{-4}) is required to trigger the system to self-sustained oscillations than is required for white noise.

As well as triggering the system from the zero solution to the

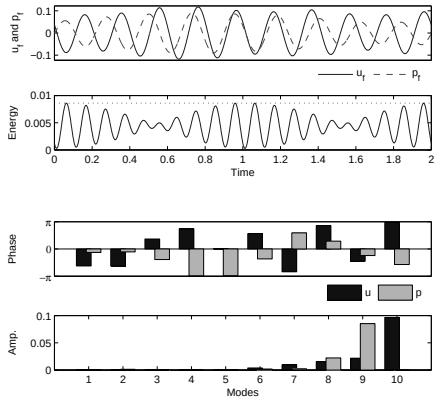

Figure 8: Blue noise with energy 8.6×10^{-3} (as for Fig. 6)

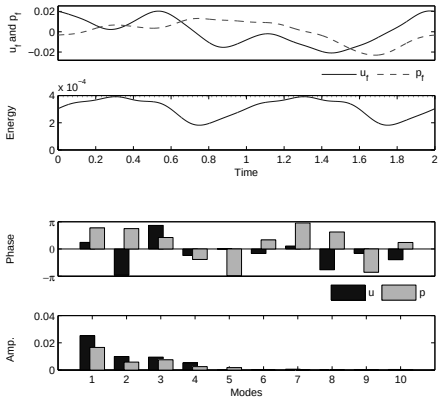

Figure 10: Pink noise with energy 3.92×10^{-4} (as for Fig. 6)

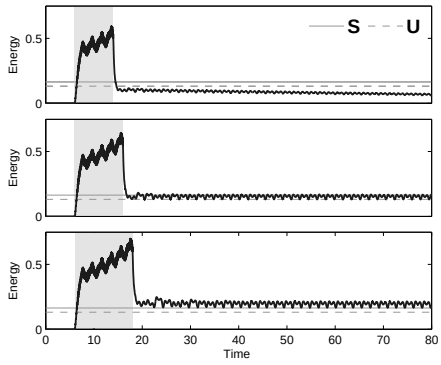

Figure 9: As for Fig. 7 but for blue noise.

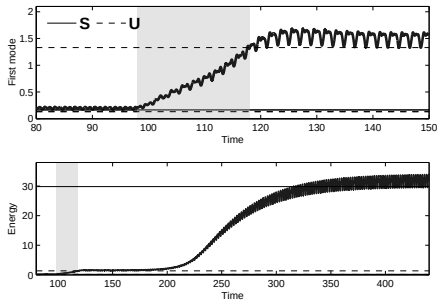

Figure 11: Energy evolution of the system with a 10 period burst of pink noise (shaded), showing transition from the lower stable PS (S) to the higher stable PS (S) via the higher unstable PS (U).

lower stable PS, noise can trigger the system from the lower stable PS to the upper stable PS. An example of this is shown for the pink noise profile in Fig. 10 with maximum energy 3.92×10^{-4}, applied for 10 periods. This corresponds to velocity and pressure perturbations of less than $\pm 2.2\%$ at the wire. The evolution of acoustic energy is shown in Fig. 11. The top plot shows the jump from the lower stable PS (solid line) to the higher unstable PS (higher dashed line) during the time when the noise is applied (shaded). The bottom plot shows the subsequent evolution from the higher unstable PS to the higher stable PS in the absence of noise. As expected from §3, it takes very little energy for pink noise to trigger the system to the higher stable PS.

In summary, pink noise is more effective at triggering to the stable PSs than white noise, which in turn is more effective than blue noise. Noise can cause triggering from the zero solution to the stable PSs, as well as from the lower to the higher stable PS. Very little noise is required, particularly if it leaves the system in a similar state to the 10 lower energy points in §3, which will grow transiently to the unstable PS. In more complex thermoacoustic systems, where the degree of non-normality and transient growth is higher [4], the latter effect will be more pronounced. Such rapid triggering to high energy oscillations through the action of low energy noise has been seen in experimental combustors, such as in Lieuwen [15, Fig. 15].

It is worth noting that additive noise can also reduce the system's acoustic energy, particularly when added to the higher Galerkin modes. This is as expected from the 10 higher energy points in §3.

4.2. Continuous noise

Continuous noise is more representative of a real system than the bursts of noise studied in §4.1 but the analysis in §3, which was for a noiseless system, is less applicable. Continuous noise was added to the system in a similar manner to §4.1 and as before, pink noise was the most effective for triggering to the high stable PS, and blue noise was the least effective.

5. Conclusions

This paper explores the analogy between triggering in thermoacoustics and bypass transition in hydrodynamics. The behaviour of a simple thermoacoustic system [3, 10] is compared with that of simplified models of hydrodynamic systems [2, 5, 6, 7]. In the thermoacoustic system, it is shown that initial

states over a wide energy range evolve first towards an unstable attractor and then towards a stable solution, which is either periodic or zero. Some of these states have lower energy than the lowest energy on the unstable attractor and make use of non-normal transient growth to reach it, which is directly analogous to bypass transition in hydrodynamics. These initial states have higher amplitudes at low frequencies.

In light of this analogy, this paper then explores the effect that different types of noise have on triggering. Three types of noise are considered: pink noise (higher amplitudes at low frequencies), white noise (similar amplitudes at all frequencies) and blue noise (higher amplitudes at high frequencies). The noise is applied both as short bursts and continuously. In both cases, pink noise is more effective than white noise, which is more effective than blue noise, at causing triggering to a higher stable periodic solution. Indeed, blue noise can even inhibit triggering. These results concur with the results in the first part of the paper. The noise signature of flames has been shown to be pink in nature [16], so these results are pertinent for ducted flame systems.

In hydrodynamics, non-normal transient growth is a key part of bypass transition, and explains why flows that have no unstable eigenvalues become turbulent with small perturbations. In thermoacoustics, triggering is directly analogous to bypass transition and therefore non-normal transient growth could play an important role. Even though the thermoacoustic system examined in this paper is only slightly non-normal, it exhibits significant transient growth towards an unstable attractor. This is likely to be even more important in more realistic thermoacoustic systems, which are significantly more non-normal [4].

References

[1] T. C. Lieuwen, V. Yang, Combustion instabilities in gas turbine engines, AIAA, 2005.
[2] P. Schmid, D. S. Henningson, Stability and transition in shear flows, Springer, 2001.
[3] K. Balasubramanian, R. I. Sujith, Physics of Fluids 20 (2008) 044103.
[4] K. Balasubramanian, R. I. Sujith, Journal of Fluid Mechanics 594 (2008) 29–57.
[5] J. Skufca, J. Yorke, B. Eckhardt, Physical Review Letters 96 (2006) 5–8.
[6] T. Schneider, B. Eckhardt, J. Yorke, Physical Review Letters 99 (2007) 1–4.
[7] Y. Duguet, A. P. Willis, R. R. Kerswell, Journal of Fluid Mechanics 613 (2008) 255–274.
[8] N. Noiray, D. Durox, T. Schuller, S. Candel, Journal of Fluid Mechanics 615 (2008) 139–167.
[9] F. Nicoud, L. Benoit, C. Sensiau, T. Poinsot, AIAA Journal 45 (2007) 426–441.
[10] M. Juniper, Submitted to Journal of Fluid Mechanics (2009).
[11] A. Dowling, J. Ffowcs-Williams, Sound and Sources of Sound, Ellis Horwood, 1983.
[12] K. Engelborghs, T. Luzyanina, D. Roose, ACM Transactions on Mathematical Software 28 (2002) 1–21.
[13] P. Ashwin, M. Timme, Nonlinearity 18 (2005) 2035–2060.
[14] P. Clavin, J. S. Kim, F. A. Williams, Combustion Science and Technology 96 (1994) 61–84.
[15] T. Lieuwen, Journal of Propulsion and Power 18 (2002) 61–67.
[16] R. Rajaram, T. Lieuwen, Combustion Science and Technology 175 (2003) 2269–2298.